Understanding of the Retarded Oxidation Effects in Silicon Nanostructures

Christophe Krzeminski, Xiang-Lei Han, Guilhem Larrieu

Understanding of the Retarded Oxidation Effects in Silicon Nanostructures

C. Krzeminski and X.-L. Han

IEMN-UMR CNRS 8520, Département ISEN,

Avenue poincaré, 59650 Villeneuve d'Ascq, France[*]

G. Larrieu

LAAS/CNRS, Université de Toulouse, 7,

av. du Colonel Roche 31077 Toulouse Cedex 4, France[†]

(Dated: March 13, 2012)

Abstract

In-depth understanding of the retarded oxidation phenomenon observed during the oxidation of silicon nanostructures is proposed. The wet thermal oxidation of various silicon nanostructures such as nanobeams, concave/convex nanorings and nanowires exhibits an extremely different and complex behavior. Such effects have been investigated by the modeling of the mechanical stress generated during the oxidation process explaining the retarded regime. The model describes the oxidation kinetics of silicon nanowires down to a few nanometers while predicting reasonable and physical stress levels at the Si/SiO_2 interface by correctly taking into account the relaxation effects in silicon oxide through plastic flow.

[*] christophe.krzeminski@isen.fr

[†] guilhem.larrieu@laas.fr

Retarded oxidation where the oxide growth slows down very rapidly with oxidation duration or with the silicon nanoobject dimension is still a puzzling physical effect [1–3]. This physical effect can be viewed as a technological nanoscale tool able to control the nanoobjects shape, size distribution interface properties and could be used in many applications [4]. However, only very few studies have been dedicated to the understanding of the phenomenon which remains fragmented and limited [5–7]. In this work, oxidation kinetics have been investigated both on the experimental and theoretical counterparts in order to improve the understanding of the mechanisms of retarded mechanisms and to quantify the amount of stress generated at the Si/SiO_2 interface in silicon nanostructures.

With the current top-down fabrication capabilities, etched silicon nanostructures including nanobeams, nanorings and nanowires have been fabricated with a high resolution [8] and then wet oxidized at 850°C. The seminal work of Kao *et al.* [9, 10] with micrometer size of 2D cylindric object is revisited but in the nanometric range. Experimentally, the oxidation kinetics have been observed to be strongly dependent on the size and the geometry of the nanoobject. Fig. 1.a) summarizes the evolution of the oxide thickness as a function of the oxidation duration in the case of convex (SiNWs) and concave (Si nanorings) structures. The oxide growth rate is strongly limited with the oxidation time but is faster in a convex structure than in a concave one. The influence of the geometrical effect is stronger with smaller inner radius (i.e. 70 nm compared to 430 nm). For the convex case, a higher oxide growth rate is related to the larger radii. Then, in order to investigate experimentally the influence of silicon nanostructure dimension, nanobeams and nanowires of height 240 nm have been oxidized for 10 and 20 minutes. As shown in insert 1.b).(1), a non-uniform oxide growth is classically observed along the sidewall of the beam due to the great influence of the top and bottom corners corresponding to a convex and concave structure respectively. An oxidized one-dimensional nanostructure with diameters from 40 nm to 140 nm demonstrated completely different shapes as shown in insert 1.b).(2) with the presence of a pinching effect at the bottom of Si nanobeam structures. In order to compare the oxidation between the two structures, the oxide thicknesses have been measured in the middle of these vertical structures described in SEM images and are plotted in Fig. 1.b). The oxide growth on Si nanobeams of previous width L is clearly thicker than a SiNWs with the diameter $d = L$. A size dependent oxidation kinetic was not observed in these structures whatever the nanobeam width considered. These experimental results illustrate

that the silicon oxidation retarded mechanism is strongly dependent at the nanoscale level on the nanoobject i) dimension ii) size and iii) shape.

These dependences cannot be explained by the standard Deal and Grove oxidation model [11], as for example, a larger oxidant concentration for the smallest particles should in principle lead to a higher oxidation rate. Two main theories have been put forward to explain the retarded/self-limiting kinetics factor. The first one is the "stress limited reaction rate" assumption [6] with a radial stress build-up at the Si/SiO_2 interface assumed to be linearly dependent of the oxidation time up to a critical stress estimated to a few GPa where the oxidation rate would be completely negligible. The second theory is the "diffusion limited mechanism" associated to a significant increase in the activation energy of the oxidant diffusivity in the highly stressed region is put forward [2]. In this framework, the origin of self-limited effects would be the oxidant species supply at the interface. Despite the fact that an unknown and uncontrolled amount of strain is introduced, no quantitative determination of the mechanical stress build-up during processing is provided by the two approaches.

In order to model the oxidation of cylinder nanoobjects, the extended Deal and Grove model in cylindrical coordinates has been used [10]. The wet oxidation rate v at the Si/SiO_2 interface is given by (Eq. 1) :

$$v = \frac{(\alpha - 1)C^*}{N} \cdot \frac{1}{\frac{1}{k_{Si}^{\sigma}} \pm \frac{a}{D^p} \log(\frac{b}{a})} \tag{1}$$

with respectively a (b) the inner (outer) radius, α the volume expansion factor of silicon to oxide conversion (2.25), N the number of oxidant molecules incorporated into a unit volume of silicon oxide, the + (resp. -) sign denotes the convex (concave) surface. This equation classically takes into account that the surface curvature influences the oxidant concentration and in the convex (concave) configuration, the concentration increases (decreases). In our approach, both the reaction rate k_{Si}^{σ} at the Si/SiO_2 interface and the diffusivity in the silicon oxide D_{SiO_2} are stress dependent. The reaction rate k_{Si}^{σ} is directly proportional to the linear rate constant $(B/A)_{[110]}(T)$ ($5.18\ 10^{-09}$ nm/s at 850°C) defined in the Deal and Grove approach by introducing C^* the oxidant solubility in the silicon dioxide and is strongly dependent on the radial stress component σ_r at the Si/SiO_2 interface :

$$k_{Si}^{\sigma} = \frac{N}{C^*} \cdot (B/A)_{[110]}(T) \exp\left(\frac{\sigma_r V_k}{k_B T}\right) \tag{2}$$

where k_B is the Boltzmann constant, T is the oxidation temperature and V_k (15 Å^3) corresponds to the activation volume. A compressive radial stress ($\sigma_r < 0$) slows down the linear rate oxidation rate. The term $(B/A)_{[110]}(T)$ takes into account the influence of the [110] crystalline orientation and the factor taking into account orientation effects has been calibrated with planar bulk oxidation experiments. Next the oxidant diffusivity, D_{SiO_2} :

$$D_{SiO_2} = \frac{N}{2C^*} \cdot B(T) = \frac{N}{2C^*} \cdot B_0(T) \cdot \exp\left(\frac{-PV_d}{k_B T}\right) \tag{3}$$

is linearly dependent on the initial parabolic constant $B_0(T)$ (2.68 10^{-13} nm^2/s at 850°C) and is limited by a compressive ($P > 0$) hydrostatic pressure $P = -0.5 \cdot (\sigma_r + \sigma_\theta)$ in the silicon oxide (V_d=45 Å^3). These assumptions are often estimated to be equivalent to a diffusivity dependence with oxide density [12].

A major issue in oxidation modelling is a proper description of the mechanical behavior of silicon dioxide as shown, in Fig. 2, and its ability to store or to dissipate mechanical energy. A shortcoming is also observed for the viscous standard approach [10, 13] since the compressive radial stress at the interface is inversely proportional to the curvature radius of the nanoobject and strongly overestimates the stress level [14]. The main reason is that the irreversible atomic rearrangements occurring with large shearing forces [15] are neglected. This plastic flow can been described by a shear dependent viscosity [16] :

$$\eta(\tau) = \eta_0(T) \frac{\tau/\sigma_c}{\sinh(\tau/\sigma_c)} \tag{4}$$

where $\eta_0(T)$ is the low stress viscosity, τ is the critical resolved shear stress and σ_c is the critical stress threshold where plasticity flow should appear (1 GPa). The low stress viscosity value (1.4 10^{18} Poisse at 850°C) considered is characteristic of a wet oxide with a high viscosity induced by the presence of hydroxyl content [17]. Following the expression of the critical resolved shear stress $\tau(r) = \frac{2\eta a \nu}{r^2}$, it can be underlined that the oxidation growth rate (Eq. 1), the shear dependent viscosity (Eq. 2) and finally the critical shear stress are coupled to each others. The fact that all of these equations must be self-consistently solved is often overlooked or not exactly taken into account. Following Rafferty *et al.* [18], the radial (σ_r) and tangential (σ_θ) stress field component in the silicon dioxide of a cylinder structure (see Fig. 1.b) can be expressed as :

$$\begin{cases} \sigma_r(r) = \pm\frac{1}{2}\sigma_c\left[\left(\ln\frac{R^2}{b^2}\right)^2 - \left(\ln\frac{R^2}{r^2}\right)^2\right] \\ \sigma_\theta(r) = \sigma_r(r) - 2\tau(r) \end{cases} \quad (5)$$

with the reduced parameter $R = \sqrt{\frac{4\eta_0 av}{\sigma_c}}$. Compared to a standard viscous approach [10] with a constant viscosity, the radial stress build-up has a logarithmic dependence on the curvature radius which gives us the opportunity to model the oxidation of cylinder shape nanostructures.

Fig. 3.a) shows that the influence of the concave or convex character on the oxidation kinetics can be well predicted by the model. As shown in Fig. 3.b) a substantial non-linear increase is observed for the compressive radial stress component at the Si/SiO_2 interface up to a few GPa, coupled with an initial tensile hydrostatic pressure (inset Fig. 3.b). The radial stress build-up is not linear with time as assumed in a previous study [6]. These elements clearly indicate that a reaction limited process takes place in the convex configuration. The situation is totally different in the concave case where a radial compressive stress build-up remains limited whereas the compressive hydrostatic pressure clearly impacts the oxidant diffusivity. In that case, the major limiting factor is the diffusion mechanism which reduces the oxidant supply. A quasi self-limited oxidation for 70 nm concave structure is observed and can be correlated to the occurrence of both a diffusion and reaction limited regime. As summarized by table I, the dominant retardation mechanism is strongly dependent on the surface shape but can be explained by the variation of the stress field component at the Si/SiO_2 in agreement with previous results [10].

Fig. 4.a) presents the linear rate modeling with oxidation duration and SiNW diameters reported in Fig 1.b). A strong decrease in the reaction rate with radial stress build-up as a function of SiNW diameters is predicted which could be directly correlated to the large radial stress build up depicted in Fig. 4.c). Large non-linear build-up as a function of the oxidation time and SiNW diameters for the compressive radial stress down to 4 GPa which remains compatible with interfacial stress estimated using contact-resonance atomic force microscopy [19]. This effect causes the initial retarded effects observed in the oxidation of convex nanostructures. These simulations explain well the difference in terms of behavior between the nanobeams and the nanowires since finite elements simulations estimate a much

lower compressive stress build-up in the nanobeam. On the other hand, Fig. 4.b) presents the evolution of the parabolic rate with SiNW diameters. A decrease in the parabolic rate is observed after a significant delay which can be correlated to the tangential stress relaxation as shown in inset of Fig. 4.c). This diffusion limited effect generated by a compressive hydrostatic pressure is probably much more difficult to control as a time and diameter dependence is observed in Fig. 4.b).

In summary, retarded oxidation kinetics have been investigated at the nanoscale level for different silicon nanoobjects. We have demonstrated the influence of the nanoobject dimension, size and shape on the oxidation behavior. All of these effects have been correlated to the interfacial stress build-up during oxidation. Given the deformation rate level, modelling aspects show that plastic relaxation needs to be considered in order to estimate i) a physical mechanical stress build-up at the interface and ii) the interface velocity. Both reaction or diffusion limited mechanisms must be considered to desccribe retarded oxidation effects in silicon nanostructures.

ACKNOWLEDGEMENT

This work was partially supported by the European Commission through the NANOSIL Network of Excellence (FP7-IST-216171) and the RTB platform (French national nanofabrication network).

---

[1] R. Okada and S. Iijima, Applied Physics Letters **58**, 1662 (1991).

[2] H. I. Liu, D. K. Biegelsen, F. A. Ponce, N. M. Johnson, and R. F. W. Pease, Applied Physics Letters **64**, 1383 (1994).

[3] H. Coffin, C. Bonafos, S. Schamm, N. Cherkashin, G. B. Assayag, A. Claverie, M. Respaud, P. Dimitrakis, and P. Normand, Journal of Applied Physics **99**, 044302 (2006).

[4] X. Tang, C. Krzeminski, A. Lecavelier des Etangs-Levallois, Z. Chen, E. Dubois, E. Kasper, A. Karmous, N. Reckinger, D. Flandre, L. A. Francis, J.-P. Colinge, and J.-P. Raskin, Nano Letters **11**, 4520 (2011).

[5] D. Shir, B. Z. Liu, A. M. Mohammad, K. K. Lew, and S. E. Mohney, Journal of Vacuum Science & Technology B: Microelectronics and Nanometer Structures **24**, 1333 (2006).

[6] H. Heidemeyer, C. Single, F. Zhou, F. E. Prins, D. P. Kern, and E. Plies, Journal of Applied Physics **87**, 4580 (2000).

[7] C. C. Büttner and M. Zacharias, Applied Physics Letters **89**, 263106 (2006).

[8] X.-L. Han, G. Larrieu, P.-F. Fazzini, and E. Dubois, Microelectronic Engineering **88**, 2622 (2011).

[9] D.-B. Kao, J. McVittie, W. Nix, and K. Saraswat, Electron Devices, IEEE Transactions on **34**, 1008 (1987).

[10] D.-B. Kao, J. McVittie, W. Nix, and K. Saraswat, Electron Devices, IEEE Transactions on **35**, 25 (1988).

[11] B. E. Deal and A. S. Grove, Journal of Applied Physics **36**, 3770 (1965).

[12] P. Sutardja and W. Oldham, Electron Devices, IEEE Transactions on **36**, 2415 (1989).

[13] V. Senez, D. Collard, B. Baccus, and J. Lebailly, Journal of Applied Physics **43**, 720 (1994).

[14] C. S. Rafferty, L. Borucki, and R. W. Dutton, Applied Physics Letters **54**, 1516 (1989).

[15] M. L. Falk and J. S. Langer, Annual Reviews **2**, 353 (2011).

[16] H. Eyring, The Journal of Chemical Physics **4**, 283 (1936).

[17] G. Hetherington, K. H. Jack, and J. C. Kennedy, Physics and Chemistry of Glasses **5**, 130 (1964).

[18] C. S. Rafferty and R. W. Dutton, Applied Physics Letters **54**, 1815 (1989).

[19] G. Stan, S. Krylyuk, A. V. Davydov, and R. F. Cook, Nano Letters **10**, 2031 (2010), pMID: 20433162.

TABLE I. Main physical mechanism governing the retarded or self-limited oxidation with decreasing convex or concave nanobjects size.

Character	σ_r	P	Origin
Convex	$\nearrow$	$\ll$	Limited reaction rate
Concave	$\ll$	$\nearrow$	Limited diffusion mechanism

FIGURES CAPTION

Fig. 1: (a) Convexity vs concavity: the various symbols present the experimental oxide thickness for SiNWs (convex nanostructure) with diameters 70 nm, 130 nm and silicon nanorings (concave nanostructure) with inner diameters of 70 nm and 430 nm as a function of the oxidation time (b) Oxide thickness in the middle edge of the Si nanobeams and SiNWs for 10 min and 20 min at 850°C. The experimental trend is described by the dashed lines. Inset SEM images: (1) the Si nanobeams (cross-section view), (2) SiNWs (titled view) after oxidation where the position set to measure the oxide thickness is reported.

Fig. 2: Schematics of the concave and convex cylinder nanostructure oxidation and resulting stress field in the silicon oxide. The strain in the oxide could be divided into two components the deviatoric part associated to shape modification and the dilatational part often neglected. Plasticity effects are introduced by considering a non-linear shear dependent viscosity $\eta(\tau)$.

Fig. 3: (a) Modelling of the convex/concave oxidation kinetics using the plastic model. b) Evolution of the theoretical radial stress σ_r at the Si/SiO_2 interface. Inset provides the hydrostatic pressure evolution during the oxidation for the different nanostructures.

Fig. 4: (a) Linear rate variation with SiNW diameters showing the impact of the radial stress in the initial oxidation regime as the main limiting factor. (b) Highlight of the diffusion limited regime which takes place only when a sufficient oxide thickness has been grown. (c) Compressive radial stress build-up with decreasing SiNW diameters. Inset: tangential stress relaxation.

FIGURES

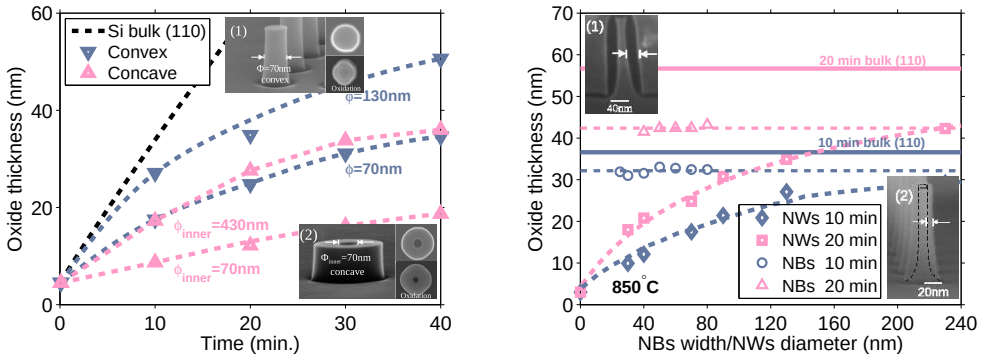

(a) (b)

FIG. 1.

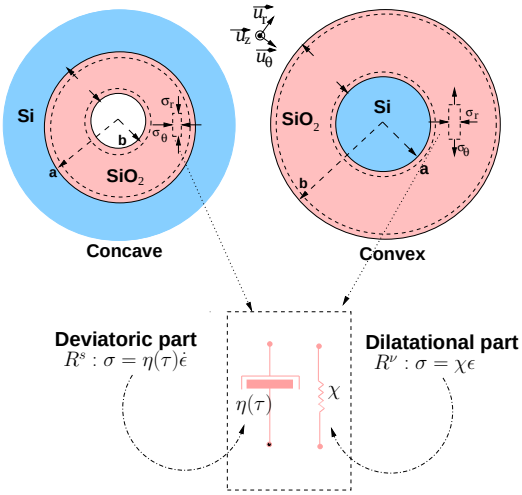

FIG. 2.

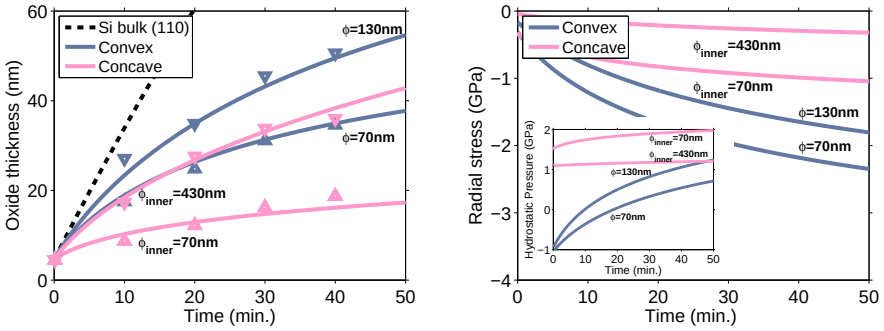

(a) (b)

FIG. 3.

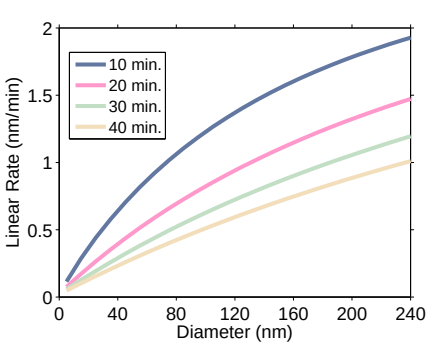
Linear Rate (nm/min)
Diameter (nm)
10 min.
20 min.
30 min.
40 min.

(a)

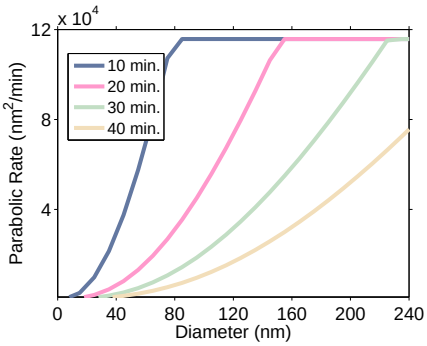
x 10^4
Parabolic Rate (nm^2/min)
Diameter (nm)
10 min.
20 min.
30 min.
40 min.

(b)

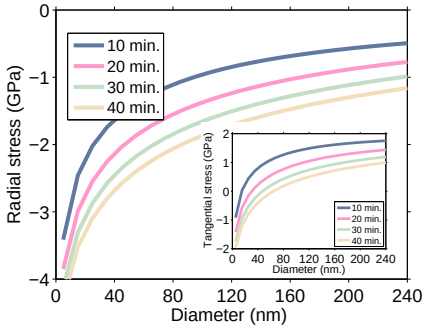
Radial stress (GPa)
Diameter (nm)
10 min.
20 min.
30 min.
40 min.
Tangential stress (GPa)
Diameter (nm.)

(c)

FIG. 4.